



Published in final edited form as:

Transl Res. 2020 April ; 218: 16–28. doi:10.1016/j.trsl.2019.12.002.

Quantitative Efficacy Paradigms of the Influenza Clinical Drug Candidate EIDD-2801 in the Ferret Model

Mart Toots¹, Jeong-Joong Yoon¹, Michael Hart¹, Michael G Natchus², George R Painter^{2,3}, Richard K Plemper^{1,*}

¹Institute for Biomedical Sciences, Georgia State University, Atlanta, GA 30303, USA

²Emory Institute for Drug Development, Emory University, Atlanta, GA 30322, USA

³Department of Pharmacology, Emory University, Atlanta, GA 30322, USA

Abstract

Seasonal influenza viruses cause major morbidity and mortality worldwide, threatening in particular older adults and the immunocompromised. Two classes of influenza therapeutics dominate current disease management, but both are compromised by pre-existing or rapidly emerging viral resistance. We have recently reported a novel ribonucleoside analog clinical candidate, EIDD-2801, that combines potent antiviral efficacy in ferrets and human airway epithelium cultures with a high barrier against viral escape. In this study, we established fundamental EIDD-2801 efficacy paradigms against pandemic and seasonal influenza A virus (IAV) strains in ferrets that can be used to inform exposure targets and treatment regimens. Based on reduction of shed virus titers, alleviation of clinical signs, and lowered virus burden in upper and lower respiratory tract tissues, lowest efficacious oral dose concentrations of EIDD-2801, given twice daily, were 2.3 and 7 mg/kg of body weight against seasonal and pandemic IAVs, respectively. The latest opportunity for initiation of efficacious treatment was 36 hours after infection of ferrets. Administered in 12-hour intervals, three 7 mg/kg doses of EIDD-2801 were sufficient for maximal therapeutic benefit against a pandemic IAV and significantly shortened the time to resolution of clinical signs. Ferrets infected with pandemic IAV and treated following the minimally efficacious EIDD-2801 regimen demonstrated significantly less shed virus and inflammatory cellular infiltrates in nasal lavages, but mounted a robust humoral antiviral response after recovery that was indistinguishable from that of vehicle-treated animals. These results provide an experimental basis in a human disease-relevant influenza animal model for clinical testing of EIDD-2801.

Introduction

Influenza affects approximately 10% of the world population each season, resulting in 3–5 million severe illnesses and more than 600,000 fatalities [1]. While infection with seasonal influenza viruses usually results in relatively benign symptoms in healthy adults, it causes significant morbidity and mortality in the elderly, young children and the immunocompromised [2]. Vaccines are available, but their efficacy is limited, especially

*Correspondence to: rplemper@gsu.edu.

when antigenic drifts or reassortments occur. For instance, efficacy of the vaccine was below 25% against the H3N2 virus during the 2017/2018 season, but the prevalence of that strain in the US was above 80%, resulting in a high disease burden [3]. Moreover, a growing body of literature suggests that the effectiveness of the vaccine may wane over an influenza season, leading to reduced protection towards the end of the season [4–6]. Therefore, antivirals are much needed to improve disease management especially in high-risk patients, and to increase preparedness for possible future influenza pandemics.

Four drug classes have been clinically developed over the last decades for the treatment of influenza: the M2 ion channel blockers, the NA neuraminidase inhibitors, a PA endonuclease inhibitor, and a polymerase inhibitor. The M2 inhibitor amantadine was the first drug approved for the treatment of influenza A virus infections, but it is no longer recommended since essentially all circulating strains possess pre-existing resistance to the drug [7–9].

Neuraminidase inhibitors (NAI) such as oseltamivir and zanamivir substantially shorten the duration of influenza-like illnesses in healthy adults, but an analysis of 107 clinical studies revealed that the NAIs provide no statistically significant benefit to children suffering from influenza [10]. Moreover, a meta-analysis of the 2009/2010 influenza season suggested that NAI treatment provides little benefit to hospitalized patients suffering from complicated influenza and enhances the risk of progression to severe disease such as viral pneumonia [11]. Resistance to NAI inhibitors is well documented, and even though it is relatively rare in the currently circulating influenza strains [12], up to 90% of the circulating strains exhibited resistance to NAIs during the 2007/2008 and 2008/2009 influenza seasons [13–15].

Baloxavir marboxil, the founding member of the novel PA endonuclease inhibitor class, was recently licensed in Japan and the United States for the treatment of uncomplicated influenza in patients greater than 12 years of age. The efficacy of baloxavir marboxil is similar or better than that of the NAIs. The drug is administered only once and is active against viruses containing signature resistance mutations to the NAIs [16, 17]. Although preexisting resistance to baloxavir marboxil appears to be rare at present [18], resistant viruses emerged in 9.7% of participants in one of the first clinical trials [17]. Viruses with reduced susceptibility to baloxavir marboxil were furthermore detected in approximately 20% of participants in a pediatric study in Japan [19]. These resistant viruses appeared to transmit efficiently and prolonged symptomatic disease by approximately 13 hours (63.1 versus 49.6 hours) compared to that in patients harboring viruses without resistance mutations [17]. Although viruses with signature mutations in PA (I38T or I38M) showed reduced replicative fitness *in vitro* [19], this penalty apparently does not translate equally to the *in vivo* setting [20, 21].

Favipiravir (T-705) is a broad-spectrum pyrazinecarboxamide that is converted by host enzymes into a ribonucleoside analog. The inhibitor is conditionally licensed in Japan for the treatment of viruses resistant to other influenza drugs. The efficiency of anabolism of ribosylated favipiravir to its active 5'-triphosphate form is low in certain disease-relevant tissues including human airway epithelium [22] and its use is associated with teratogenicity and embryotoxicity [23]. The barrier to resistance against favipiravir was originally assumed to be insurmountable [24], but more recent work has revealed a route to escape based on two

compensatory mutations [25, 26]. Considering the challenges experienced by the currently approved therapeutics, well-tolerated, efficacious next-generation influenza virus inhibitors with a high barrier against resistance are needed.

We have recently demonstrated that the ribonucleoside analog *N*⁴-hydroxycytidine (NHC, EIDD-1931) is a broad-spectrum inhibitor of seasonal and highly pathogenic influenza A as well as influenza B viruses [22]. However, the clinical use of NHC may be compromised by poor oral bioavailability, which was observed in non-human primate models. To overcome this limitation, we have identified a 5'-isopropylester prodrug of NHC, EIDD-2801, which shows greatly improved pharmacokinetic properties including good oral bioavailability in cynomolgus macaques and ferrets [27]. We showed that the drug is efficacious against influenza A and B viruses in disease-relevant differentiated 3D human airway epithelium models and ferrets under therapeutic dosing conditions. In addition, we demonstrated that a high barrier exists against influenza virus escape from inhibition. Mechanistically, the drug induces random low-frequency C-U and G-A transitions resulting in viral error catastrophe [27].

In the present study, we determined efficacy cornerstones of EIDD-2801: the minimal efficacious dose, the latest onset of effective treatment, and the minimum number of doses required for maximum effect. These critical parameters were determined in the ferret model of influenza infection, which is considered the most relevant model for preclinical drug development [28, 29], since it recapitulates hallmarks of human influenza disease.

Methods

Cells and viruses

Madin-Darby canine kidney (MDCK) cells (ATCC CCL-34) were grown at 37°C and 5% CO₂ in Dulbecco's modified Eagle's medium (DMEM) supplemented with 7.5% fetal bovine serum (FBS). A/California/07/2009 (H1N1) and A/Wisconsin/67/2005 (H3N2) were propagated on MDCK cells for 3 days at 37°C and 5% CO₂. Culture supernatants were collected, cleared by centrifugation (3,000 g for 20 min at 4°C) and stored in aliquots at -80°C. Infectious virus titers were determined by TCID₅₀-HA assay described [22].

Intranasal infection of ferrets

Ferrets 6 to 8 months of age from Marshall Bioresources or Triple F Farms were housed in an ABSL-2 facility and acclimated for at least 4 days prior to experimentation. The animals were weighed, assigned to groups randomly and anesthetized with dexmedetomidine/ketamine prior to intranasal infection with Ca/09 or with Wi/05. EIDD-2801 was administered in 3.5 ml doses in 1% methylcellulose and chased with canine liquid high calorie dietary supplement via oral gavage. Animals in control groups received volume-equivalents of vehicle only. Animals were anesthetized once every 24 hours for blood collection. Nasal lavages were obtained from, and oral gavages administered to, non-anesthetized animals. Cells in nasal lavage and white blood cells stained with Turk's solution were counted using a hemocytometer. Specific infection conditions and experimental setup for each experiment are visualized schematically in individual figures.

Animal body temperature monitoring

Body temperature was monitored using telemetric sensors (e-Celsius Medical monitoring system from BodyCap Medical), which were inserted per os to anesthetized animals at the time of influenza infection. Infectious viral titers were measured by TCID₅₀-HA assay as described [22].

Hemagglutination inhibition (HI) antibody titers

Serum was collected 0, 3, 7, 10, and 14 days after infection and treated overnight at 37°C with receptor destroying enzyme (RDE II; Accurate Chemical) at a 1:3 ratio to inactivate non-specific HA inhibitors. All reactions were stopped through heat inactivation of enzymes (56°C for 30 minutes). Treated serum samples were serially diluted in 2-fold steps in assay plates, followed by addition of an equal volume of Ca/09 (approximately 8 HAU units/well). Plates were incubated at room temperature for 20 minutes, and subsequently 50 µl/well of 0.5% chicken red blood cells added and incubation continued for an additional 30–60 minutes. HI titers were determined as the reciprocal of the highest serum dilution that completely prevents hemagglutination (described in [30]).

Immunohistochemistry

Nasal turbinates were fixed with 10% neutral-buffered formalin for 24 hours, followed by decalcification for 5 days (nasal turbinates only), embedding into paraffin blocks, and sectioning. Slides were deparaffinized and antigens recovered using HistoReveal (Abcam). Endogenous biotin was blocked by incubating the slides in 0.001% biotin-PBS for 10 minutes, followed by 10-minute incubation in 0.001% avidin-PBS. After blocking with 10% BSA Blocker (Thermo Scientific), slides were incubated with specific anti-IAV HA antiserum at 4°C, washed twice with PBS, and incubated with biotinylated conjugate antibody. Signal was detected using the ABC Peroxidase Staining Kit (Thermo Scientific) according to the manufacturer's instructions and DAB staining with hematoxylin counterstaining.

Minigenome assay

293T cells were transfected in a 96-well plate format with Ca/09-derived expression plasmids encoding PB1 (standard or with K229R substitution), PB2, PA (standard or with P659L substitution), NP, and a plasmid containing a nano-luciferase reporter gene flanked by influenza A virus untranslated regions (UTRs) as described [31]. Parallel transfections lacking the PB2 expression vector served as negative controls. Three-fold serial dilutions of inhibitor (100 µM highest concentration) were added to the cells three hours post-transfection using a Nimbus automated liquid handler, followed by incubation for 24 hours. Nano-luciferase reporter activity was measured using an HI Synergy multimode plate reader (BioTek), and was expressed relative to vehicle controls. Four-parameter variable slope regression modeling was applied to calculate 50% inhibitory concentrations ((EC₅₀s) using the Prism software package (GraphPad).

Statistics

GraphPad Prism software was used for all statistical analyses. 1-way or 2-way ANOVA with Dunnett's or Sidak's multiple comparisons post-hoc tests were used to evaluate statistical significance when more than two groups were compared or datasets contained two independent variables, respectively. The specific test applied to individual studies is specified in figure legends. Results obtained for individual biological replicates are shown in each figure, along with mean or median values as specified in figure legends. Experimental uncertainties are expressed as standard deviation (SD). Continuously monitored body temperature data from all animals in a study group were subjected to Lowes analyses, and statistical time-to-event (body temperature below 39°C fever cut-off) determined through Mantel-Cox test. For all experiments, the statistical significance level α was set to <0.05, exact P values are shown in individual graphs.

Ethics statement

The study conforms to the relevant ethical guidelines for human and animal research. All animal work was performed in compliance with the Guide for the Care and Use of Laboratory Animals of the National Institutes of Health as well as the Animal Welfare Act Code of Federal Regulations. All experimentation involving ferrets was approved by the Georgia State University Institutional Animal Care and Use Committee (IACUC) under protocol A18035.

Results

Minimal efficacious dose of EIDD-2801 against pandemic Ca/09 in ferrets

In previous work, we have determined pharmacokinetic and anabolism profiles of EIDD-2801 in ferrets, among other species, and correlated ferret pharmacokinetic prodrug profiles with intracellular drug concentrations in human disease-relevant fully differentiated human airway epithelia cultures. Extrapolations based on these studies predicted that 7 mg/kg of EIDD-2801 administered orally b.i.d. would yield sustained tissue concentrations of the bioactive 5'-triphosphate form of the drug, sufficient for near-sterilizing anti influenza virus activity without off-target effects [27]. We have furthermore validated experimentally that 7 mg/kg of EIDD-2801 administered orally b.i.d. is efficacious in the ferret model against pandemic A/California/07/2009 (H1N1) (Ca/09) [27]. To explore the boundaries of compound potency and inform clinical testing, we performed a minimal efficacious dose finding study in ferrets. Ferrets were infected intranasally with Ca/09 and treated b.i.d. with 7, 2.3 or 0.8 mg/kg EIDD-2801 (Fig 1A). Treatment with a 7 mg/kg EIDD-2801 oral dose led to reduction of shed virus load by several orders of magnitude (Fig 1B), recapitulating the results of our previous work. In contrast, the 2.3 mg/kg dose resulted in moderate reduction of virus titer in nasal lavages (Fig 1B), but no significant reduction of fever, the predominant clinical marker in ferrets, was observed (Fig 1C). Independent of treatment, Ca/09-infected ferrets did not show signs of respiratory distress (sneezing, wheezing) and no changes in body weight of untreated infected versus uninfected animals were noted (Supplementary Figure 1). Oral dosing of EIDD-2801 at 0.8 mg/kg had no significant therapeutic effect. Similar to shed viral load, virus titers in the upper respiratory tract were significantly lower in the animals that had received 7 mg/kg of EIDD-2801, whereas

treatment with a 2.3 mg/kg dose did not reduce titers significantly compared to vehicle-treated animals (Fig 1D). Interestingly, viral load in the lower respiratory tract was significantly reduced in animals that had received EIDD-2801 at either a 7 or a 2.3 mg/kg dose (Fig 1E-G). However, dosing at 0.8 mg/kg had no significant effect on virus burden in the large and small airways (Fig 1F). Coinciding with antiviral activity, cellular infiltrates in the nasal cavities as well as white blood cell counts remained unchanged in animals of the 7 mg/kg dose group throughout the study, whereas 2.3 mg/kg EIDD-2801 had only a moderate effect (Fig 1H-I). Although treatment at the 2.3 mg/kg dose reduced viral burden slightly, it did not shorten the duration of fever. These results identify 7 mg/kg as the lowest efficacious oral dose of EIDD-2801, when administered following a b.i.d. dosing regimen.

Latest onset of treatment with EIDD-2801 against Ca/09 in ferrets

Our previous study has shown that therapeutic treatment with EIDD-2801 initiated 24 hours post-infection (after the onset of clinical signs and at peak viral shedding) effectively reduces viral load and shortens the duration of clinical signs in the ferret model [27]. To determine the latest time point after infection for the initiation of efficacious treatment, we infected ferrets intranasally with Ca/09 as outlined in Fig 2A and started treatment with the minimal efficacious EIDD-2801 dose, 7 mg/kg, 36 or 48 hours post-infection. In either case, dosing was continued b.i.d. until five days after infection. Viral shedding from the upper respiratory tract was measured every 12 hours throughout the course of the study. Whereas treatment initiated 36 hours post-infection significantly reduced viral titers in nasal lavage compared to that in vehicle-treated animals, no therapeutic benefit was observed in the 48-hour treatment group (Fig. 2B). The impact of treatment on viral shedding was directly reflected by reduced viral loads in the nasal turbinates (Fig 2C), trachea (Fig 2D) and in the bronchial lavage (Fig 2E) of the 36-hour treatment group. No statistically significant differences were observed in the 48-hour treatment group compared to the vehicle group. These data underscore the robust efficacy of EIDD-2801 and demonstrate that a 36-hour time window exists for the onset of effective treatment with EIDD-2801 after infection.

Minimal number of doses required for efficacious treatment

We have previously demonstrated that doses of EIDD-2801 of up to 100 mg/kg b.i.d. are well tolerated in ferrets over several days without increased random transition mutation frequencies in nuclear and mitochondrial RNA in cells of the respiratory tract [27]. Nevertheless, reducing host drug exposure to the minimum required for full therapeutic benefit is paramount to avoid adverse effects. Having established the minimal efficacious EIDD-2801 dose, we queried the minimum number of doses required for efficacy. Initially starting treatment 12 hours after infection with Ca/09 (Fig 3A), ferrets received one or two doses of EIDD-2801 at 7 mg/kg. Whereas virus shedding was transiently alleviated in both groups, no significant reduction of viral titers in nasal turbinates and lung was detected (Fig 3B-D) and fever was only moderately reduced without significant shortening of overall duration (Fig 3E). In contrast, administration of three and four doses at the same dose concentration significantly reduced viral load in nasal lavages (Fig 3F) and both the upper and lower respiratory tract (Fig 3G-H), resulting in overall therapeutic benefit similar to that seen after continuous b.i.d. dosing for the full course of the study (Fig 1 and [27]). Drug was first administered to animals of the three-dose and four-dose groups 24 hours after infection.

Consistent with effective reduction of virus load, three administrations of EIDD-2801 also significantly shortened the duration of fever (Fig 3I), confirming that treatment with three doses of the drug, started at the peak of virus shedding and continued in 12-hour intervals, is sufficient for full therapeutic benefit.

Validation of efficacy parameters through immunohistochemistry

To further validate the minimal efficacious dose and number of doses, we monitored virus spread to nasal turbinates *in situ* through immunohistochemistry. Nasal turbinates of vehicle-treated animals showed massive virus invasion and high concentration of viral antigen in the epithelial cell layer (Fig 4A and B). Treatment initiated 36 hours after infection at the 7 mg/kg dose concentration almost completely eliminated viral antigen, whereas first drug administration 48 hours after infection had no appreciable effect (Fig 4A), consistent with the quantitation of viral tissue load after these treatment regimens (Fig 2). Likewise, immunohistochemistry corroborated that three doses of EIDD-2801 initiated 24 hours after infection are sufficient for robust suppression of virus replication, returning effect sizes similar to those observed after four doses (Fig 4B) or a full drug course over the duration of the study [27].

Humoral response to Ca/09 after minimally efficacious EIDD-2801 treatment course

Our initial characterization of EIDD-2801 focused on therapeutic benefit in the setting of acute disease, covering mostly the first days after infection [27]. To assess whether treatment affects the adaptive antiviral immune response of the host, we monitored cellular infiltrates into the upper respiratory tract and neutralizing antibody titers over an extended time period (up to 2-weeks) time period (Fig. 5A). For this study, the minimal efficacious dose and minimal number of doses was administered to the Ca/09-infected ferrets, i.e. three doses of EIDD-2801 at the 7 mg/kg dose, initiated 24 hours after infection and given according to a b.i.d. regimen. Treatment significantly reduced shed virus titers as noticed in previous studies, although the overall duration of virus shedding was not shortened, and virus became undetectable in both treated and vehicle animals by day seven after infection (Fig 5B). No late-onset signs of respiratory distress such as sneezing or wheezing were observed in this 2-week study period. Coinciding with lower virus burden in the upper respiratory tract, inflammatory cellular infiltrates in nasal lavages were significantly lower in treated animals compared to the vehicle control group (Fig 5C). Most importantly, the kinetics and extent of the humoral response to influenza virus infection in treated and vehicle animals were indistinguishable, resulting in robust HI titers detectable by day 7 after infection (Fig 5D). These data confirm that the drug alleviates virus-induced inflammation, but treated animals mount a robust, protective humoral response against the challenge virus.

Effect of resistance mutations to favipiravir on polymerase sensitivity to EIDD-2801

A K229R mutation in the PB1 subunit of the influenza virus polymerase complex mediated resistance of a pandemic 2009 H1N1 influenza virus to favipiravir in minigenome assays and recombinant virus, albeit with the penalty of impaired viral fitness [25]. However, fitness could be restored through a compensatory P653L substitution in the PA polymerase subunit, resulting in an approximately 30-fold reduction in sensitivity of the double mutant virus to favipiravir compared to its genetic parent [25]. To assess whether this mutation pair

causes cross-resistance with EIDD-2801, we rebuilt both substitutions in a Ca/09-derived minigenome system and determined the inhibitory activity of NHC, the hydrolysis product of EIDD-2801, in dose-response assays (Fig 6). EC₅₀ concentrations of NHC against standard and mutant polymerase complexes differed by less than 2-fold and no increase in EC₉₀ concentrations of the mutant was detected, indicating that resistance to favipiravir does not coincide with escape from EIDD-2801.

Treatment with minimal efficacious dose of EIDD-2801 against seasonal Wi/05 in ferrets

We have established that EIDD-2801 is efficacious against seasonal H3N2 influenza viruses, representing group 2 HA subtype IAVs [27]. To explore whether the lowest efficacious EIDD-2801 dose determined for pandemic Ca/09 equally applies to seasonal virus, we infected ferrets intranasally with A/Wisconsin/67/2005 (H3N2) (Wi/05) strain and initiated treatment 24 hours after infection at doses of 7, 2.3, 0.8, and 0.3 mg/kg EIDD-2801 (Fig 7A). In this assessment, treatment was continued in a b.i.d. regimen until study end after the first dose. Against seasonal Wi/05, doses of 2.3 and 7 mg/kg were sufficient to reduce viral loads in nasal lavages and turbinates to levels close to or below the detection limit, respectively, within 12 hours of the initial dose (Fig 7B). Dose concentrations of less than 2.3 mg/kg had only a transient (0.8 mg/kg) effect on viral burden or were not effective (0.3 mg/kg) (Fig 7B-C). Reflecting the lower pathogenicity of seasonal Wi/05 in the ferret model, duration and severity of fever was moderate compared to challenge with Ca/09, confounding efficacy assessment based on alleviation of clinical signs (Fig 7D). However, treatment at the 2.3 and 7 mg/kg doses completely suppressed cellular infiltrates into the upper respiratory tract (Fig 7E) and alleviated a virus-induced increase in total white blood cell counts (Fig 7F) that was previously observed in H3N2-infected ferrets [32, 33]. These results reveal that efficacious dose cut-offs established for a pdm09 IAV strain can be extended with considerable margin to seasonal IAV of different HA subtype group.

Discussion

In this study, we have dosed the recently identified anti-influenza virus clinical candidate EIDD-2801 to failure to establish critical parameters defining the scope of antiviral efficacy: the lowest efficacious dose, the minimal number of doses required for efficacy, and the latest time point after infection for initiation of efficacious therapy. Different animal models of influenza infection have been established and are routinely used for pre-clinical drug candidate testing, although their predictive value of drug performance in humans varies. For instance, the IAV/mouse model is still most commonly used for influenza drug evaluation [34, 35], despite its poor recapitulation of some fundamental aspects of human infection. Among these, mice do not support productive infection with most human strains without prior virus adaptation, first viral replication takes place predominantly in the lower, rather than upper, respiratory tract, and, consistent with predominant infection of the small airways, viral shedding is low and transmission between animals inefficient [28, 29, 36, 37]. These discrepancies in host invasion and disease progression compared to human infection directly impair the predictive value of fundamental efficacy parameters extracted from the mouse model, especially with respect to the latest onset of efficacious treatment and minimal numbers of doses required for maximum benefit.

The ferret model better addresses these concerns, since ferrets are naturally susceptible to human influenza A and B viruses, viral replication occurs initially predominantly in the upper respiratory tract, and ferrets efficiently shed virus in high titers and exhibit human-like relatively mild clinical signs of disease such as fever. Only infection with highly pathogenic avian influenza viruses results in severe lethargy and loss of body weight [38–40]. The recapitulation of hallmarks of human influenza improves confidence that efficacy paradigms established for EIDD-2801 in ferrets will provide a viable basis to define clinical expectations.

Specifically, we have determined that treatment with EIDD-2801 doses of 7 mg/kg administered b.i.d. is sufficient for antiviral efficacy against pdm09 H1N1 and seasonal H3N2 influenza strains in ferrets, corresponding to an approximate daily human dose equivalent of 2.6 mg/kg, when considering standard species conversion estimates [41]. We have no evidence that Wi/05 is inherently more sensitive to inhibition by EIDD-2801 than Ca/09, since EC₅₀ and EC₉₀ values, determined in both human primary differentiated airway epithelium models and immortalized cell lines, were very similar against both strains [22, 27]. Rather, the lower minimal efficacious doses against Wi/05 in ferrets (2.3 vs. 7 mg/kg) most likely reflects the lower pathogenicity of the seasonal H3N2 in the model, coinciding with substantially lower peak virus load and moderate clinical signs compared to Ca/09, consistent with previous reports [42].

Multi-dose administration of EIDD-2801 was well-tolerated by different animal species, but the possible impact of the compound on fetal health is unknown at present. Taking teratogenicity and embryotoxicity of favipiravir into account [23], possible adverse effects on fetal health must be evaluated experimentally before use of the compound for influenza therapy during pregnancy can be considered.

In the case of rapidly replicating viruses associated predominantly with acute disease, such as influenza, the anticipated time windows for the initiation of efficacious treatment are narrow. First administration of licensed therapeutics such as the neuraminidase inhibitors or baloxavir marboxil is recommended within 48 hours of the appearance of symptoms [34, 43–45], but experimental data suggests that the actual period of opportunity may be substantially shorter and limited to approximately 24 hours or less in humans [46, 47]. No experimental data have been released for the window of opportunity of baloxavir marboxil in animal models, but neuraminidase inhibitors must be administered within approximately 24 hours of infection in ferrets to achieve any therapeutic benefit, although reduction of viral load in ferrets was minimal in general after therapeutic dosing [46, 48, 49]. In light of these limitations of licensed therapeutics, our identification of a significant, quantitative therapeutic benefit when treatment was started 36 hours after infection is encouraging, placing EIDD-2801 on par with, or ahead of, existing therapeutics.

In addition to a reasonable time window for the onset of treatment, patient compliance is strongly impacted by the necessary dosing regimen and the number of doses required for efficacy [50–52]. Our previous multi-species PK studies have demonstrated that EIDD-2801 must be taken twice daily to ensure sustained efficacious drug levels in disease-relevant respiratory tissues [27]. However, we demonstrate here that a standard treatment course can

very likely be limited to 1.5 days (3 oral doses), which in our opinion greatly alleviates concerns regarding the compliance of non-hospitalized patients suffering from seasonal influenza, a primary patient target population for EIDD-2801, may be limited. Importantly, our data indicate that patients receiving this drug regimen will not only profit from direct antiviral activity of EIDD-2801 but can be expected to experience fewer immunopathogenic pro-inflammatory complications associated with influenza virus infection and ultimately mount a strong, protective adaptive antiviral immune response.

Taken together, our recent proof-of-concept efficacy study identifying EIDD-2801 as an anti-influenza clinical candidate and the present evaluation of quantitative efficacy parameters provide strong support for the further advancement of the compound to clinical testing for human influenza therapy.

Supplementary Material

Refer to Web version on PubMed Central for supplementary material.

Acknowledgements

We thank MT Saindaine and MA Lockwood for chemical syntheses, and AL Hammond for critical reading of the manuscript. No further editorial support was used. All authors have read the journal's policy on disclosure of potential conflicts of interest. MGN and GRP hold patent 20190022116, "N⁴-Hydroxycytidine and Derivatives and Anti-Viral Uses Related Thereto", covering composition of matter and method of use of EIDD-2801 for influenza therapy. This study could affect their personal financial status. All other authors declare no competing interests. All authors have read the journal's authorship agreement. The manuscript has been reviewed by and approved by all named authors. This work was supported, in part, by Public Health Service grants AI071002 (to RKP) and AI141222 (to RKP), from the NIH/NIAID. The funders had no role in study design, data collection and interpretation, or the decision to submit the work for publication.

References

- [1]. Rolfes MA, Foppa IM, Garg S, Flannery B, Brammer L, Singleton JA, et al. Annual estimates of the burden of seasonal influenza in the United States: A tool for strengthening influenza surveillance and preparedness. *Influenza Other Respir Viruses*. 2018;12:132–7. [PubMed: 29446233]
- [2]. Littmann J. How high is a high risk? Prioritising high-risk individuals in an influenza pandemic. *Vaccine*. 2014;32:7167–70. [PubMed: 25454881]
- [3]. Garten R, Blanton L, Elal AIA, Alabi N, Barnes J, Biggerstaff M, et al. Update: Influenza Activity in the United States During the 2017–18 Season and Composition of the 2018–19 Influenza Vaccine. *MMWR Morb Mortal Wkly Rep*. 2018;67:634–42. [PubMed: 29879098]
- [4]. Osterholm MT, Kelley NS, Sommer A, Belongia EA. Efficacy and effectiveness of influenza vaccines: a systematic review and meta-analysis. *Lancet Infect Dis*. 2012;12:36–44. [PubMed: 22032844]
- [5]. Belongia EA, Simpson MD, King JP, Sundaram ME, Kelley NS, Osterholm MT, et al. Variable influenza vaccine effectiveness by subtype: a systematic review and meta-analysis of test-negative design studies. *Lancet Infect Dis*. 2016;16:942–51. [PubMed: 27061888]
- [6]. Costantino V, Trent M, MacIntyre CR. Modelling of optimal timing for influenza vaccination as a function of intraseasonal waning of immunity and vaccine coverage. *Vaccine*. 2019;37:6768–75. [PubMed: 31521411]
- [7]. Shiraishi K, Mitamura K, Sakai-Tagawa Y, Goto H, Sugaya N, Kawaoka Y. High frequency of resistant viruses harboring different mutations in amantadine-treated children with influenza. *J Infect Dis*. 2003;188:57–61. [PubMed: 12825171]

- [8]. Abed Y, Goyette N, Boivin G. Generation and characterization of recombinant influenza A (H1N1) viruses harboring amantadine resistance mutations. *Antimicrob Agents Chemother.* 2005;49:556–9. [PubMed: 15673732]
- [9]. Krumbholz A, Schmidtke M, Bergmann S, Motzke S, Bauer K, Stech J, et al. High prevalence of amantadine resistance among circulating European porcine influenza A viruses. *J Gen Virol.* 2009;90:900–8. [PubMed: 19223487]
- [10]. Jefferson T, Jones MA, Doshi P, Del Mar CB, Hama R, Thompson MJ, et al. Neuraminidase inhibitors for preventing and treating influenza in healthy adults and children. *Cochrane Database Syst Rev.* 2014:CD008965.
- [11]. Muthuri SG, Myles PR, Venkatesan S, Leonardi-Bee J, Nguyen-Van-Tam JS. Impact of neuraminidase inhibitor treatment on outcomes of public health importance during the 2009–2010 influenza A(H1N1) pandemic: a systematic review and meta-analysis in hospitalized patients. *J Infect Dis.* 2013;207:553–63. [PubMed: 23204175]
- [12]. Lee N, Hurt AC. Neuraminidase inhibitor resistance in influenza: a clinical perspective. *Curr Opin Infect Dis.* 2018;31:520–6. [PubMed: 30299356]
- [13]. Dharan NJ, Gubareva LV, Meyer JJ, Okomo-Adhiambo M, McClinton RC, Marshall SA, et al. Infections With Oseltamivir-Resistant Influenza A(H1N1) Virus in the United States. *JAMA-J Am Med Assoc.* 2009;301:1034–41.
- [14]. Hurt AC, Ernest J, Deng YM, Iannello P, Besselaar TG, Birch C, et al. Emergence and spread of oseltamivir-resistant A(H1N1) influenza viruses in Oceania, South East Asia and South Africa. *Antivir Res.* 2009;83:90–3. [PubMed: 19501261]
- [15]. Esposito S, Molteni CG, Colombo C, Daleno C, Dacco V, Lackenby A, et al. Oseltamivir-induced resistant pandemic A/H1N1 influenza virus in a child with cystic fibrosis and *Pseudomonas aeruginosa* infection. *J Clin Virol.* 2010;48:62–5. [PubMed: 20335065]
- [16]. Noshi T, Kitano M, Taniguchi K, Yamamoto A, Omoto S, Baba K, et al. In vitro characterization of baloxavir acid, a first-in-class cap-dependent endonuclease inhibitor of the influenza virus polymerase PA subunit. *Antiviral Res.* 2018;160:109–17. [PubMed: 30316915]
- [17]. Hayden FG, Sugaya N, Hirotsu N, Lee N, de Jong MD, Hurt AC, et al. Baloxavir Marboxil for Uncomplicated Influenza in Adults and Adolescents. *N Engl J Med.* 2018;379:913–23. [PubMed: 30184455]
- [18]. Gubareva LV, Mishin VP, Patel MC, Chesnokov A, Nguyen HT, De La Cruz J, et al. Assessing baloxavir susceptibility of influenza viruses circulating in the United States during the 2016/17 and 2017/18 seasons. *Euro Surveill.* 2019;24.
- [19]. Omoto S, Speranzini V, Hashimoto T, Noshi T, Yamaguchi H, Kawai M, et al. Characterization of influenza virus variants induced by treatment with the endonuclease inhibitor baloxavir marboxil. *Sci Rep.* 2018;8:9633. [PubMed: 29941893]
- [20]. Chesnokov A, Patel MC, Mishin VP, De La Cruz JA, Lollis L, Nguyen HT, et al. Replicative fitness of seasonal influenza A viruses with decreased susceptibility to baloxavir. *J Infect Dis.* 2019.
- [21]. Checkmahomed L, M’Hamdi Z, Carbonneau J, Venable MC, Baz M, Abed Y, et al. Impact of the baloxavir-resistant polymerase acid (PA) I38T substitution on the fitness of contemporary influenza A(H1N1)pdm09 and A(H3N2) strains. *J Infect Dis.* 2019.
- [22]. Yoon JJ, Toots M, Lee S, Lee ME, Ludeke B, Luczo JM, et al. Orally Efficacious Broad-Spectrum Ribonucleoside Analog Inhibitor of Influenza and Respiratory Syncytial Viruses. *Antimicrob Agents Chemother.* 2018;62.
- [23]. Nagata T, Lefor AK, Hasegawa M, Ishii M. Favipiravir: a new medication for the Ebola virus disease pandemic. *Disaster Med Public Health Prep.* 2015;9:79–81. [PubMed: 25544306]
- [24]. Baranovich T, Wong SS, Armstrong J, Marjuki H, Webby RJ, Webster RG, et al. T-705 (favipiravir) induces lethal mutagenesis in influenza A H1N1 viruses in vitro. *J Virol.* 2013;87:3741–51. [PubMed: 23325689]
- [25]. Goldhill DH, Te Velhuis AJW, Fletcher RA, Langat P, Zambon M, Lackenby A, et al. The mechanism of resistance to favipiravir in influenza. *Proc Natl Acad Sci U S A.* 2018;115:11613–8. [PubMed: 30352857]

- [26]. Goldhill DH, Langat P, Xie HY, Galiano M, Miah S, Kellam P, et al. Determining the Mutation Bias of Favipiravir in Influenza Virus Using Next-Generation Sequencing. *J Virol.* 2019;93.
- [27]. Toots M, Yoon JJ, Cox RM, Hart M, Sticher ZM, Makhsous N, et al. Characterization of orally efficacious influenza drug with high resistance barrier in ferrets and human airway epithelia. *Sci Transl Med.* 2019;11.
- [28]. Bouvier NM, Lowen AC. Animal Models for Influenza Virus Pathogenesis and Transmission. *Viruses.* 2010;2:1530–63. [PubMed: 21442033]
- [29]. Mifsud EJ, Tai CMK, Hurt AC. Animal models used to assess influenza antivirals. *Expert Opin Drug Dis.* 2018;13:1131–9.
- [30]. Francis ME, McNeil M, Dawe NJ, Foley MK, King ML, Ross TM, et al. Historical H1N1 Influenza Virus Imprinting Increases Vaccine Protection by Influencing the Activity and Sustained Production of Antibodies Elicited at Vaccination in Ferrets. *Vaccines (Basel).* 2019;7.
- [31]. Weisshaar M, Cox R, Morehouse Z, Kumar Kyasa S, Yan D, Oberacker P, et al. Identification and Characterization of Influenza Virus Entry Inhibitors through Dual Myxovirus High-Throughput Screening. *J Virol.* 2016;90:7368–87. [PubMed: 27252534]
- [32]. Music N, Reber AJ, Lipatov AS, Kamal RP, Blanchfield K, Wilson JR, et al. Influenza vaccination accelerates recovery of ferrets from lymphopenia. *PLoS One.* 2014;9:e100926.
- [33]. Music N, Reber AJ, Kim JH, York IA. Peripheral Leukocyte Migration in Ferrets in Response to Infection with Seasonal Influenza Virus. *PLoS One.* 2016;11:e0157903.
- [34]. Principi N, Camilloni B, Alunno A, Polinori I, Argentiero A, Esposito S. Drugs for Influenza Treatment: Is There Significant News? *Front Med-Lausanne.* 2019;6. [PubMed: 30761303]
- [35]. Davidson S. Treating Influenza Infection, From Now and Into the Future. *Front Immunol.* 2018;9. [PubMed: 29403493]
- [36]. Lu X, Tumpey TM, Morken T, Zaki SR, Cox NJ, Katz JM. A mouse model for the evaluation of pathogenesis and immunity to influenza A (H5N1) viruses isolated from humans. *J Virol.* 1999;73:5903–11. [PubMed: 10364342]
- [37]. Dybing JK, Schultz-Cherry S, Swayne DE, Suarez DL, Perdue ML. Distinct pathogenesis of hong kong-origin H5N1 viruses in mice compared to that of other highly pathogenic H5 avian influenza viruses. *J Virol.* 2000;74:1443–50. [PubMed: 10627555]
- [38]. Oh DY, Hurt AC. Using the Ferret as an Animal Model for Investigating Influenza Antiviral Effectiveness. *Front Microbiol.* 2016;7.
- [39]. Radigan KA, Misharin AV, Chi M, Budinger GS. Modeling human influenza infection in the laboratory. *Infect Drug Resist.* 2015;8:311–20. [PubMed: 26357484]
- [40]. Stark GV, Long JP, Ortiz DI, Gainey M, Carper BA, Feng J, et al. Clinical profiles associated with influenza disease in the ferret model. *PLoS One.* 2013;8:e58337. [PubMed: 23472182]
- [41]. Nair AB, Jacob S. A simple practice guide for dose conversion between animals and human. *J Basic Clin Pharm.* 2016;7:27–31. [PubMed: 27057123]
- [42]. Huang SS, Banner D, Fang Y, Ng DC, Kanagasabai T, Kelvin DJ, et al. Comparative analyses of pandemic H1N1 and seasonal H1N1, H3N2, and influenza B infections depict distinct clinical pictures in ferrets. *PLoS One.* 2011;6:e27512.
- [43]. Roche, Announces FDA Approval of Xofluz (baloxavir marboxil) for Influenza; available online: <https://www.roche.com/media/releases/med-cor-2018-10-24.htm>. 2018.
- [44]. Cooper NJ, Sutton AJ, Abrams KR, Wailoo A, Turner DA, Nicholson KG. Effectiveness of neuraminidase inhibitors in treatment and prevention of influenza A and B: systematic review and meta-analyses of randomised controlled trials. *Brit Med J.* 2003;326:1235–+. [PubMed: 12791735]
- [45]. Kaiser L, Wat C, Mills T, Mahoney P, Ward P, Hayden F. Impact of oseltamivir treatment on influenza-related lower respiratory tract complications and hospitalizations. *Arch Intern Med.* 2003;163:1667–72. [PubMed: 12885681]
- [46]. Oh DY, Lowther S, McCaw JM, Sullivan SG, Leang SK, Haining J, et al. Evaluation of oseltamivir prophylaxis regimens for reducing influenza virus infection, transmission and disease severity in a ferret model of household contact. *J Antimicrob Chemother.* 2014;69:2458–69. [PubMed: 24840623]

- [47]. Wong ZX, Jones JE, Anderson GP, Gualano RC. Oseltamivir treatment of mice before or after mild influenza infection reduced cellular and cytokine inflammation in the lung. *Influenza Other Resp.* 2011;5:343–50.
- [48]. Govorkova EA, Marathe BM, Prevost A, Rehg JE, Webster RG. Assessment of the efficacy of the neuraminidase inhibitor oseltamivir against 2009 pandemic H1N1 influenza virus in ferrets. *Antiviral Res.* 2011;91:81–8. [PubMed: 21635924]
- [49]. Marriott AC, Dove BK, Whittaker CJ, Bruce C, Ryan KA, Bean TJ, et al. Low dose influenza virus challenge in the ferret leads to increased virus shedding and greater sensitivity to oseltamivir. *PLoS One.* 2014;9:e94090.
- [50]. Jin J, Sklar GE, Min Sen Oh V, Chuen Li S. Factors affecting therapeutic compliance: A review from the patient’s perspective. *Ther Clin Risk Manag.* 2008;4:269–86. [PubMed: 18728716]
- [51]. Martin LR, Williams SL, Haskard KB, Dimatteo MR. The challenge of patient adherence. *Ther Clin Risk Manag.* 2005;1:189–99. [PubMed: 18360559]
- [52]. Ingersoll KS, Cohen J. The impact of medication regimen factors on adherence to chronic treatment: a review of literature. *J Behav Med.* 2008;31:213–24. [PubMed: 18202907]

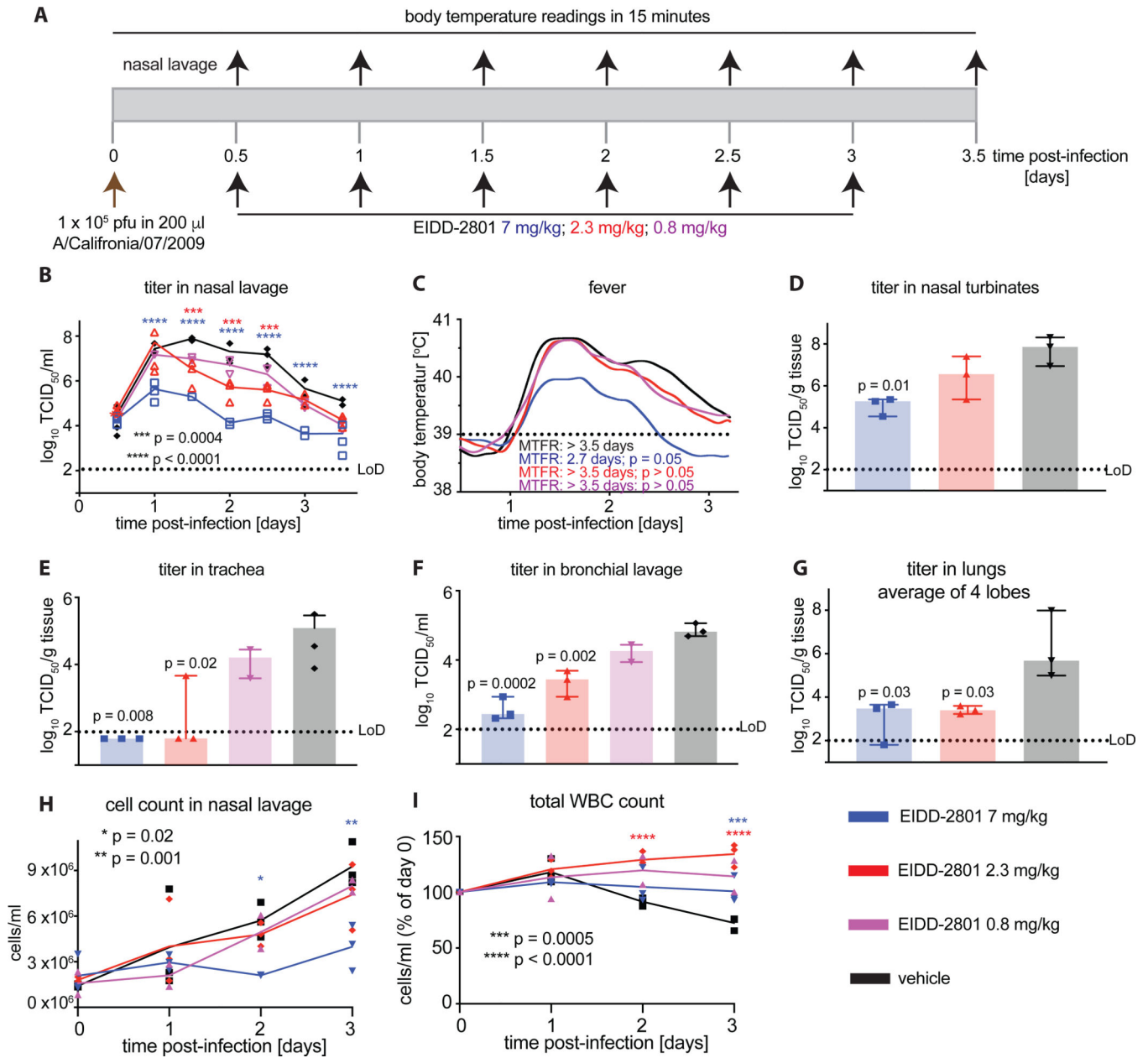


Figure 1. Minimal efficacious dose of EIDD-2801 against Ca/09. **A**) Schematic of the experimental setup. **B**) Shed virus titer in nasal lavages, taken in 12-hour intervals. **C**) Body temperature of animals continuously monitored with implanted telemetric sensors. Lowes analysis of data, statistical time-to-event (body temperature below 39°C fever cut-off) through Mantel-Cox test. MTRF – median time to fever resolve. **D–G**) Virus titer in the upper and lower respiratory tract, determined 3.5 days after infection. Tissue titers (nasal turbinates (D) and lung lobes (G)) were only determined when titers in lavages (B, E, F) revealed a significant difference to those present in vehicle-treated animals. Average virus distribution in caudal and cranial lung lobes shown in (G). **H**) Total inflammatory cell counts in nasal lavages from (B). **I**) Total white blood cell counts expressed relative to counts at the time of infection (day

0). Throughout, symbols represent biological repeats ($N = 3$ for all groups with the exception of 0.8 mg/kg, which had ($N = 2$); lines connect medians in (B) and means in (H) and (I); columns indicate medians \pm SD (range for 0.8 mg/kg). Statistical analyses by 2-way ANOVA (B, H, I) or 1-way ANOVA (D–G) with Dunnett’s multiple comparisons post-hoc test. LoD – limit of detection.

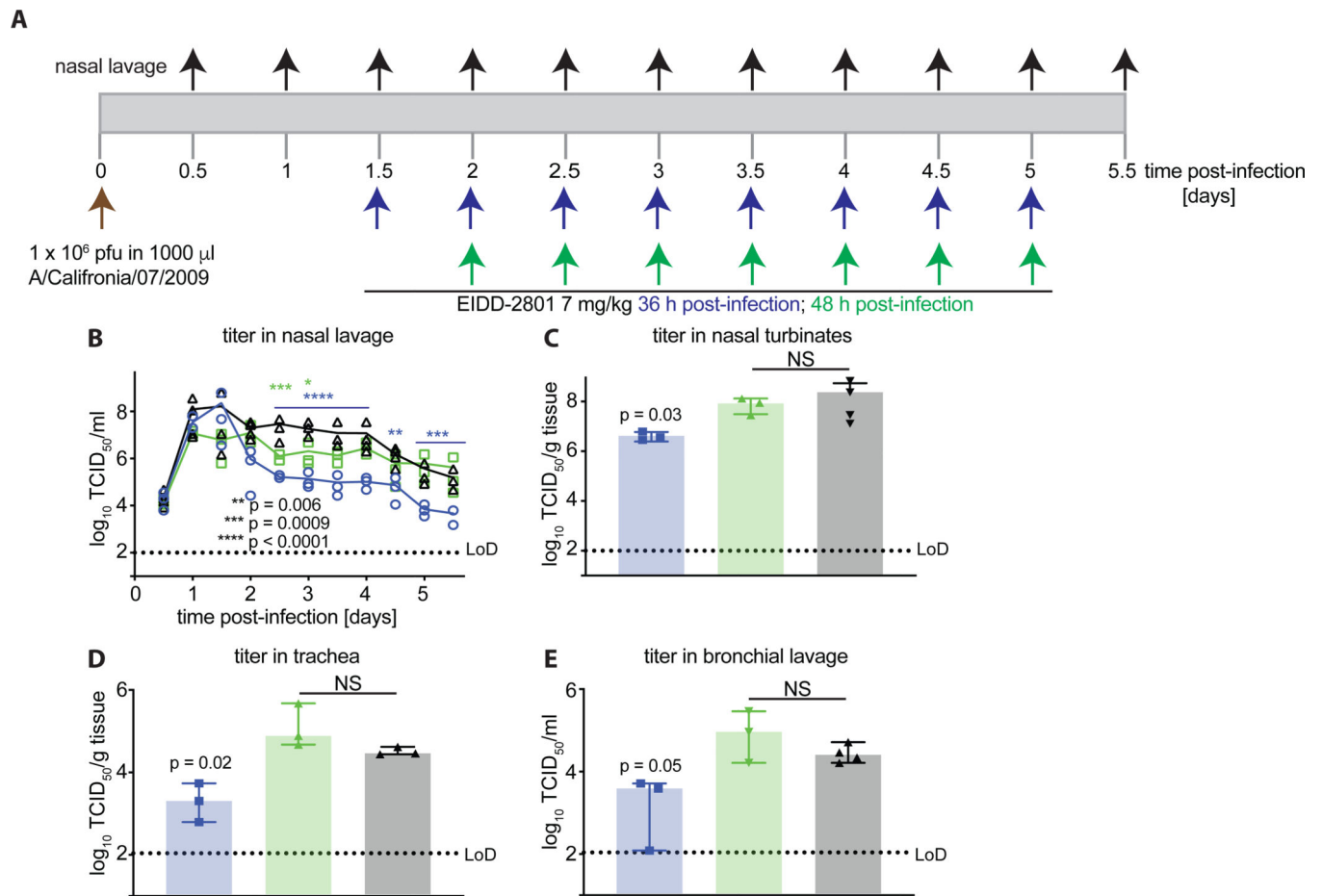


Figure 2.

Latest onset of efficacious treatment of Ca/09 infection with EIDD-2801. **A)** Schematic of the experimental setup. **B)** Shed virus titer in nasal lavages, taken in 12-hour intervals. **C–E)** Virus titer in different respiratory tissues, measured 5.5 days post-infection. Symbols represent biological repeats (N = 3–4), lines connect medians; columns indicate medians ± SD. Statistical analysis by 2-way ANOVA (B) or 1-way ANOVA (C–E) with Dunnett's multiple comparisons post-hoc test; NS: not significant.

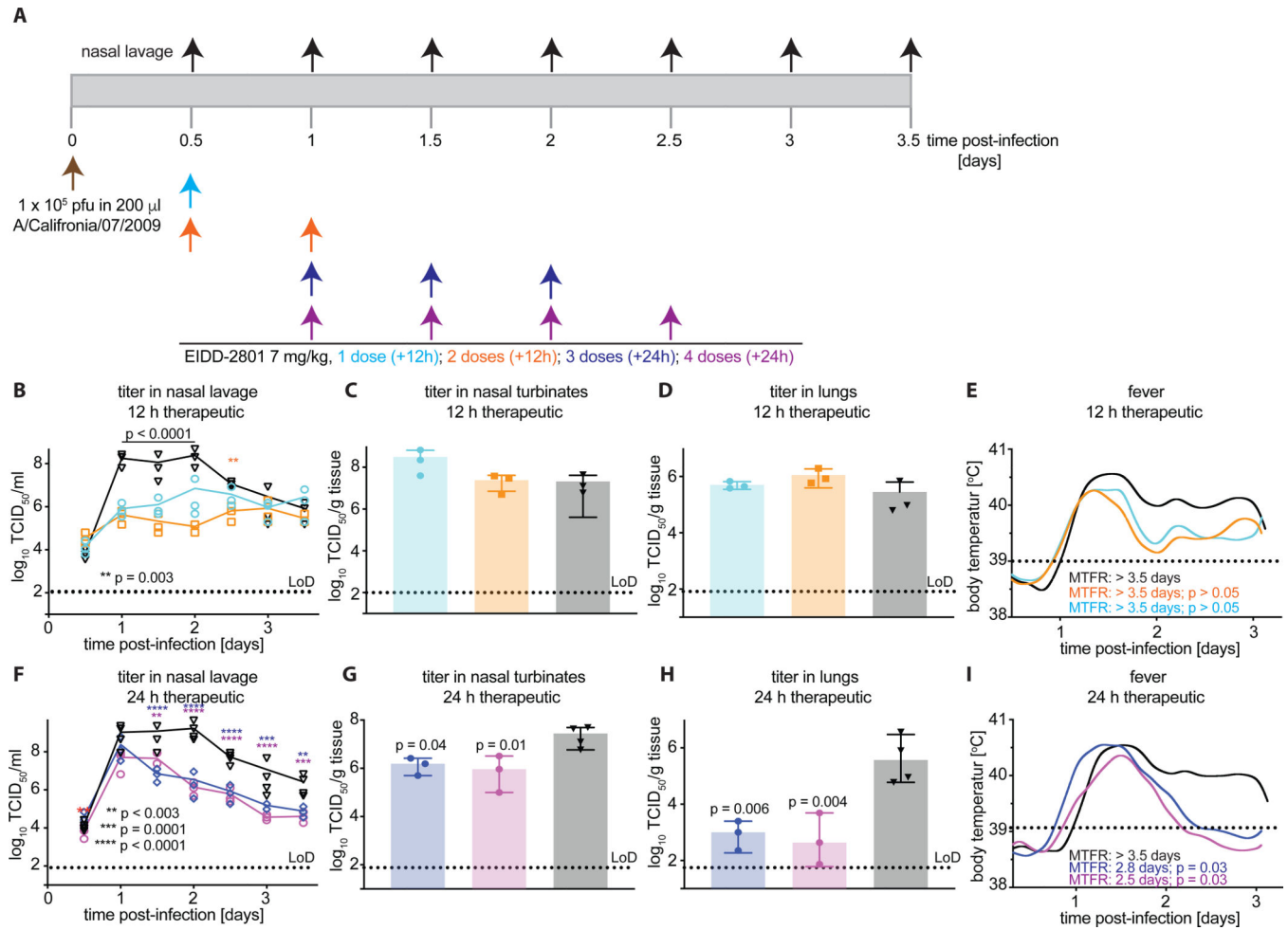


Figure 3.

Minimal number of doses required for efficacious treatment of Ca/09 infection of ferrets with EIDD-2801. **A)** Schematic of the experimental setup. **B–E)** Treatment initiated 12 hours after infection. Shed virus titer in nasal lavages, taken in 12-hour intervals (**B**). Virus titer in upper (**C**) and lower (**D**) respiratory tract tissues, measured 3.5 days after infection. Body temperature of animals (**E**), continuously monitored with implanted telemetric sensors. Analysis as in (1C). **F–I)** Treatment initiated 12 hours after infection. Assessment of animals as in (**B–E**). Symbols represent biological repeats ($N = 3–4$), lines connect medians, and columns indicate medians \pm SD. Statistical significance was determined by 2-way ANOVA (**B, F**) or by 1-way ANOVA (**C–D** and **G–H**) with Dunnett’s multiple comparisons post-hoc test.

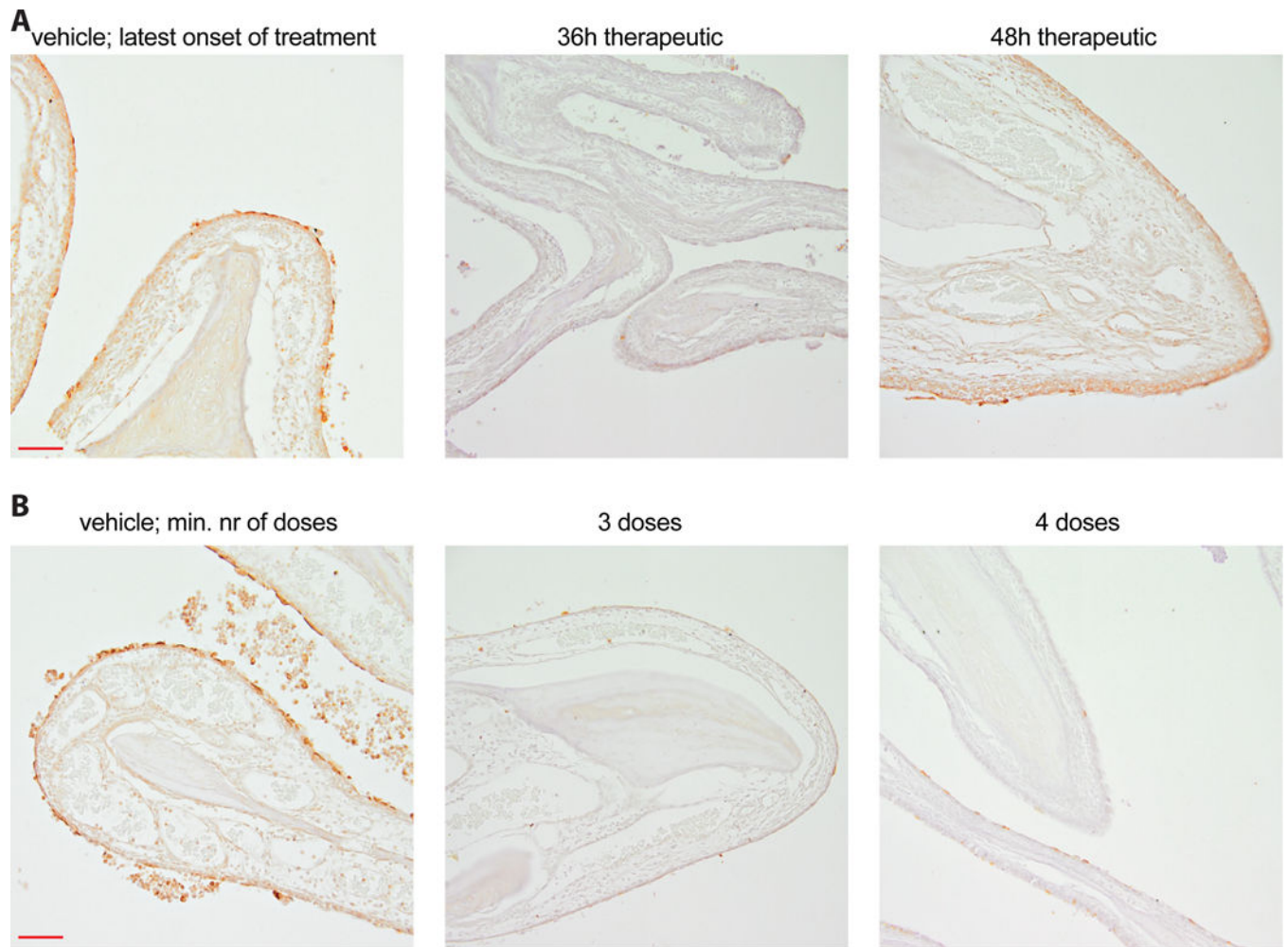


Figure 4. Immunohistochemistry of nasal turbinates extracted from ferrets in studies of the latest onset of treatment (A) and minimal number of doses required (B) studies. Representative images of tissues from vehicle and EIDD-2801-treated animals are shown. Influenza virus was detected with anti-HA antiserum and DAB staining (brown). Tissues were counterstained with hematoxylin. Scale bars represent 50 μm.

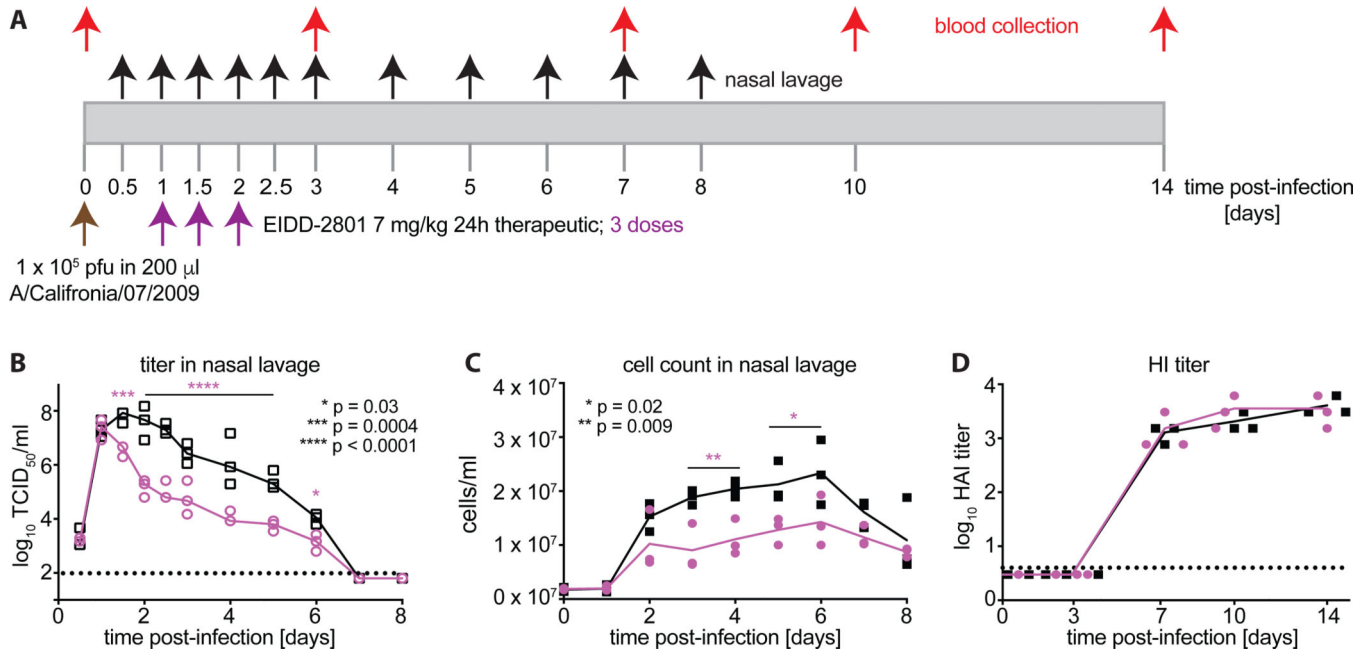


Figure 5.

Effect of EIDD-2801 treatment on viral clearance and adaptive antiviral response. **A)** Schematic of the experimental setup. **B)** Shed virus titer in nasal lavages, taken in 12-hour intervals. **C)** Inflammatory cell count in nasal lavages from (B). **D)** Hemagglutination inhibition (HI) serum antibody titers in vehicle and EIDD-2801-treated animals, determined from blood samples taken on day 0, 3, 7, 10, and 14 after infection. Serum samples were tested against the Ca/09 strain. Symbols represent biological repeats (N = 3), lines connect medians. Statistical significance was determined by 2-way ANOVA with Sidak's multiple comparisons post-hoc test.

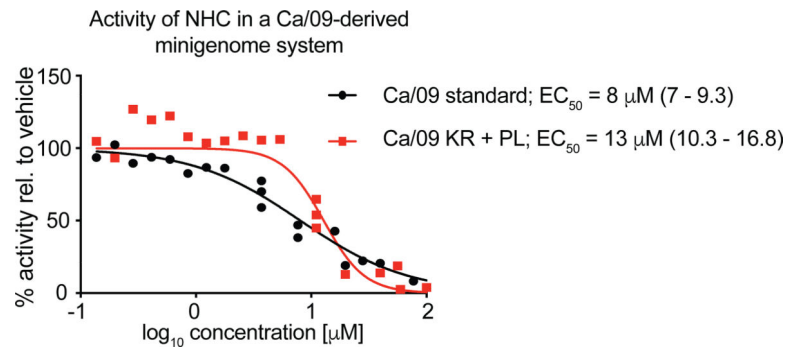


Figure 6.

Activity testing of NHC in a Ca/09-derived minigenome reporter assay, comparing unmodified polymerase complexes (Ca/09 standard) and complexes harboring two substitutions reportedly mediating resistance to favipiravir (Ca/09 KR + PL, carrying mutations PB1 K229R and PA P653L) [25, 26]. Symbols show biological repeats ($n = 3$) for each concentration tested, lines represent four-parameter variable slope regression models. EC_{50} concentrations are specified, 95% confidence intervals in parentheses.

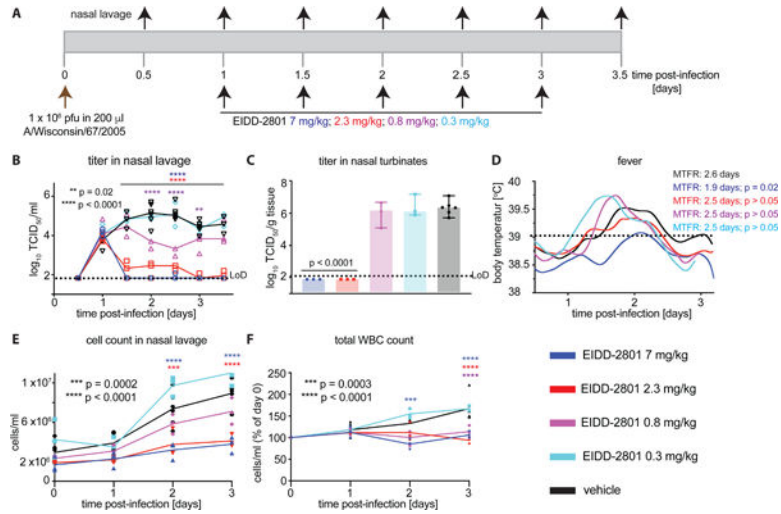


Figure 7.

Minimal efficacious dose of EIDD-2801 against seasonal Wi/05 in ferrets. **A)** Schematic of the experimental setup. **B)** Shed virus titer in nasal lavages, taken in 12-hour intervals. **C)** Virus titer in nasal turbinates, extracted 3.5 days after infection. **D)** Body temperature of animals continuously monitored with implanted telemetric sensors. Analysis as in (1C). **E)** Total inflammatory cell counts in nasal lavages from (B). **F)** Total white blood cell counts expressed relative to counts at the time of infection (day 0). Symbols are biological replicates ($N = 3$), lines connect medians (B) or means (E, F). Columns (C) show medians \pm SD. Statistical analysis by 2-way ANOVA (B, E, F) or 1-way ANOVA (C) with Dunnett's multiple comparisons post-hoc test.